Comparison between semiclassical and quantum mechanical calculations for collisional broadening and shift of HCO^+ rotational lines

G. Buffa
IPCF-CNR, Largo Pontecorvo 3, I-56127 Pisa, Italy
(Received 26 January 2007; published 12 October 2007)

For eight HCO^+ rotational transitions we compare semiclassical and quantum calculations of the line broadening and shift induced by collisions with argon and helium atoms. A detailed analysis of the results allows better insights into the problem of the accuracy of the semiclassical model commonly used in most line shape studies.

DOI: 10.1103/PhysRevA.76.042509 PACS number(s): 33.70.Jg, 33.20.Bx

I. INTRODUCTION

In the spectroscopic studies of gases, a full quantum treatment [1,2] of the effect of collisions on the line shape can be performed only for very simple molecular systems, while it is a too difficult task for most cases of practical interest. As a consequence one is frequently forced to use a theoretical approach [3–8] involving simplifying approximations: semiclassical treatment of the collision and perturbative expansion of the interaction. For sake of simplicity we will call it an Anderson-Tsao-Curnutte (ATC) approximation, including in this name also the extensions [5,6] and modifications [7,8] later introduced.

A comparison between ATC and quantum calculations is rarely performed in the literature because of two main reasons. First, they are used for different molecular species; second, they resort to different potentials: accurate potential energy surfaces are preferred for quantum calculations, while potentials made of terms going as r^{-n} are used for ATC calculations.

A comparison was realized by Hartmann and Boulet for HF-Ar [9] and by Hutson [10] for HCl-Ar. However, they did not resort to the ATC approximation, but to different semiclassical frameworks, such as the one developed by Neilsen and Gordon [11] which is more accurate than the ATC approximation, but also more complicated and is not easily applied to many molecular species of practical interest.

In the present paper we perform a detailed comparison for the rotational spectrum of the ion HCO^+ perturbed by collisions with helium and argon atoms. The choice of such perturbers is due to the availability of reliable potentials [12,13]. For both theoretical methods we can resort to the same potential energy surfaces by a reformulation of the semiclassical treatment which removes the restrictions on the potential. Our choice of dealing with a molecular ion, whose electric charge gives rise to a very-long-range interaction, allows us to investigate also the influence of the capture effect [14–17], which is particularly important in the case of collisions with argon.

II. IMPACT APPROXIMATION

All the calculations throughout this paper rely upon the impact approximation [18,19], which assumes that the collisional line shape is a Lorentzian whose width Γ and shift s are linear with perturber density n and are given by the real and imaginary parts of the cross section σ: $\Gamma - is = n\bar{v}\sigma$, where $\bar{v} = (8kT/\pi m)^{1/2}$ is the mean relative velocity and m is the reduced mass of the colliding pair. The relaxation efficiency of a collision is described by a complex function P, which can be expressed in terms of the scattering matrix S. For the case of an atomic perturber and for the rotational line $j_f \leftarrow j_i$ of a linear absorber one has

$$P(k) = 1 - \sum_{k'} \langle j_i,k|S|j_i,k'\rangle\langle j_f,k'|S^\dagger|j_f,k\rangle, \tag{1}$$

where k and k' are translation states. The scattering matrix S can be calculated from the interaction potential V:

$$S = \mathcal{O}\exp\left(-\frac{1}{\hbar}\int_{-\infty}^{+\infty} dt e^{iH_0 t/\hbar} V(t) e^{-iH_0 t/\hbar}\right), \tag{2}$$

where $\mathcal{O}$ is time-ordering operator, H_0 is the Hamiltonian of the internal degrees of freedom of the colliding molecules, and V is the collisional interaction.

III. SEMICLASSICAL CALCULATIONS AND ATC APPROXIMATION

The semiclassical approximation resorts to quantum mechanics only for the internal motions of the colliding partners while it treats classically the relative translation, which is characterized by impact parameter b and asymptotic relative velocity v. The cross section σ is obtained by integration of b and v:

$$\sigma = \frac{1}{\bar{v}}\int_0^\infty v f(v)\sigma(v) dv, \tag{3a}$$

$$\sigma(v) = \int_0^\infty 2\pi b P(b,v) db, \tag{3b}$$

where $f(v)$ is Maxwell's velocity distribution and the efficiency function P is defined by Eq. (1), which within the semiclassical approximation becomes

$$P(b,v) = 1 - \langle\langle j_i|S(b,v)|j_i\rangle\langle j_f|S^\dagger(b,v)|j_f\rangle\rangle_{\text{av}}, \tag{4}$$

where $\langle\cdots\rangle_{\text{av}}$ stands for the average of the directions.

It is worthwhile noting that the summation in Eq. (1) over the outgoing translation states disappears in Eq. (4). Within the classical path approximation, the changes of internal energy do not affect translation and the total energy is not conserved. This may be a crude approximation, especially when the translation energy is not much larger than internal energy changes—that is to say, at low temperatures and at high j values.

The most accurate form of the semiclassical approximation [11] resorts to a numerical solution of the scattering equation (2). However, this method was used only for very simple molecular systems, while further approximations are commonly used for other cases. For weak collisions, occurring at large impact parameters, the interaction $V(t)$ is assumed to be small and a lowest-order (second-order) perturbative expansion is used. This yields the efficiency function

$$\mathrm{Re}\, P^{\mathrm{weak}}(b,v) = \frac{1}{2\hbar^2}\left[\sum_{j'} \langle|\langle j_f|\breve{V}(\omega_{j_f j'})|j'\rangle|^2\rangle_{\mathrm{av}} + \sum_{j'} \langle|\langle j_i|\breve{V}(\omega_{j_i j'})|j'\rangle|^2\rangle_{\mathrm{av}} - 2\langle\langle j_i|\breve{V}(0)|j_i\rangle\langle j_f|\breve{V}(0)|j_f\rangle\rangle_{\mathrm{av}}\right], \tag{5a}$$

$$\mathrm{Im}\, P^{\mathrm{weak}}(b,v) = \frac{1}{2\hbar^2}\left[\sum_{j'} \langle|\langle j_f|\tilde{V}(\omega_{j_f j'})|j'\rangle|^2\rangle_{\mathrm{av}} - \sum_{j'} \langle|\langle j_i|\tilde{V}(\omega_{j_i j'})|j'\rangle|^2\rangle_{\mathrm{av}}\right], \tag{5b}$$

where ω is proportional to the collision-induced change of internal energy. Since the effect of vibrational transitions is negligible, one can restrict oneself to rotational transitions $j \to j'$: $\omega_{jj'} = (E_{j'} - E_j)/\hbar$. $\breve{V}(\omega)$ in Eq. (5a) is the Fourier transform of the potential

$$\breve{V}(\omega) = \int_{-\infty}^{+\infty} dt e^{i\omega t} V(t), \tag{5c}$$

while $|\tilde{V}(\omega)|^2$ in Eq. (5b) is the Hilbert transform of $|\breve{V}(\omega)|^2$:

$$|\tilde{V}(\omega)|^2 = \frac{1}{\pi}\mathrm{P}\int_{-\infty}^{\infty} d\omega' \frac{|\breve{V}(\omega')|^2}{\omega - \omega'}, \tag{5d}$$

where P denotes the principal value.

The case opposite to weak collisions is solved on plausibility grounds: when the impact parameter is small, the collision is strong and the outgoing rotational state of the absorber is assumed uncorrelated to the ingoing one. As a consequence,

$$\mathrm{Re}\, P^{\mathrm{strong}} = 1, \tag{6a}$$

$$\mathrm{Im}\, P^{\mathrm{strong}} = 0. \tag{6b}$$

As far as intermediate b values are concerned, the situation is more confused. Anderson, in his pioneering paper [3], proposed three possible solutions and different interpolation methods are used in the literature. Some authors resort to a cutoff [3–6,20–22], while more accurate results are obtained [7,8] by omitting the time order operator $\mathcal{O}$ in Eq. (2). This allows one to calculate the exponential by powers of the lowest-order term P^{weak} and yields a relaxation efficiency which has the expected trend in both limits of large and small impact parameters and, apart from minor differences, is related to P^{weak} by

$$P = 1 - e^{-P^{\mathrm{weak}}}. \tag{7}$$

We shall resort to this interpolation, giving broadening values somewhat lower than the ones obtained by the cutoff and in better agreement with experiment.

ATC calculations deal with potentials made of terms that depend on the distance as r^{-n}. This was first originated by the use of multipolar and dispersion potentials [4,6,23,24], but the same scheme was adopted also when short-range potentials were considered [8,25]: the sum of Lennard-Jones atom-atom interactions was approximated by terms of that type. For such interaction terms the time integral and the average of the orientation in Eqs. (5) can be performed obtaining explicit expressions, the resonance functions, for the ω dependence. This was done first by resorting to simplified trajectories (straight line [4] or parabolic [8]), but the same scheme was kept also when the exact classical trajectory was used [26–28]. Since this hinders using more general potentials, we follow a different path. We resort to an exact average of the directions in Eqs. (5), but we use numerical integration for orbital dynamics. From a computational point of view our method is not more complicated than the usual one, but it is suitable for any kind of potential. Here we develop it for the case of a linear absorber colliding with an atom, but it can be applied as well to other cases.

The interaction $V(r,\theta)$ is decomposed into Legendre polynomials

$$V(r,\theta) = \sum_{\lambda} V_\lambda(r) P_\lambda(\theta), \tag{8}$$

where θ is the angle between the axis of the linear absorber and the vector $\boldsymbol{r}$ connecting the centers of mass of the two colliding partners. A classical relative translation is calculated by using V_0, the spherical part of the potential. A plane motion is obtained, described by $r(t)$ and by $\psi(t)$, the angle between $\boldsymbol{r}(t)$ and the closest-approach radius $\boldsymbol{r}_0$. $r(t)$ and $\psi(t)$ are evaluated at discrete time intervals. By fast Fourier transform the integral functions

$$I_{\lambda,p,q}(\omega) = \int_{-\infty}^{\infty} dt e^{i\omega t} V_\lambda(r(t)) \sin^p \psi(t) \cos^q \psi(t) \tag{9}$$

are calculated. By an average over the angles, the three terms of Eq. (5a) can be expressed by Clebsh-Gordan and Racah coefficients and by the resonance functions F_λ:

$$\langle|\langle j|\breve{V}(\omega_{jj'})|j'\rangle|^2\rangle_{\mathrm{av}} = \sum_{\lambda} \frac{1}{2\lambda+1} F_\lambda(\omega_{jj'}) |\langle j\lambda 00|j'0\rangle|^2, \tag{10a}$$

$$\langle\langle j_i|\check{V}(0)|j_i\rangle\langle j_f|\check{V}(0)|j_f\rangle\rangle_{\mathrm{av}} = \sum_{\lambda} \frac{1}{2\lambda+1} F_\lambda(0)\langle j_i\lambda 00|j_i 0\rangle\langle j_f\lambda 00|j_f 0\rangle \times (-)^{j_i+j_f+\lambda+1}\sqrt{(2j_i+1)(2j_f+1)}W(j_i j_f j_i j_f, 1\lambda). \tag{10b}$$

The resonance functions $F_\lambda(\omega)$ are obtained by means of the Fourier integrals $I_{\lambda,p,q}(\omega)$:

$$F_1 = I^2_{1,1,0} + I^2_{1,0,1}, \tag{11a}$$

$$F_2 = I^2_{2,0,0} - 3I_{2,0,0}I_{2,0,2} + 3I^2_{2,1,1} + 3I^2_{2,0,2}, \tag{11b}$$

$$F_3 = I^2_{3,1,0} - 5I_{3,1,0}I_{3,1,2} + 6I^2_{3,0,1} - 15I_{3,0,1}I_{3,0,3} + 10I^2_{3,1,2} + 10I^2_{3,0,3}, \tag{11c}$$

$$F_4 = I^2_{4,0,0} - 10I_{4,0,0}I_{4,0,2} + \frac{35}{4}I_{4,0,0}I_{4,0,4} + 10I^2_{4,1,1} + 35I_{4,1,1}I_{4,1,3} + \frac{145}{4}I^2_{4,0,2} - 70I_{4,0,2}I_{4,0,4} + 35I^2_{4,1,3} + 35I^2_{4,0,4}, \tag{11d}$$

$$F_5 = I^2_{5,1,0} - 14I_{5,1,0}I_{5,1,2} + \frac{63}{4}I_{5,1,0}I_{5,1,4} + 15I^2_{5,0,1} + 105I_{5,0,1}I_{5,0,3} + \frac{315}{4}I_{5,0,1}I_{5,0,5} + \frac{301}{4}I^2_{5,1,2} - 189I_{5,1,2}I_{5,1,4} + \frac{805}{4}I^2_{5,0,3} - 315I_{5,0,3}I_{5,0,5} + 126I^2_{5,1,4} + 126I^2_{5,0,5}. \tag{11e}$$

Terms with $\lambda > 5$ are not reported because their contribution is negligible.

The two terms of Eq. (5b), describing the imaginary part of relaxation efficiency, are obtained by Hilbert transformation of the resonance functions:

$$\langle|\langle j|\tilde{V}(\omega_{jj'})|j'\rangle|^2\rangle_{\mathrm{av}} = \sum_{\lambda} \frac{1}{2\lambda+1}\tilde{F}_\lambda(\omega_{jj'})|\langle j\lambda 00|j' 0\rangle|^2, \tag{12a}$$

$$\tilde{F}_\lambda(\omega) = \frac{1}{\pi}\mathrm{P}\int_{-\infty}^{\infty} d\omega' \frac{F_\lambda(\omega')}{\omega-\omega'}. \tag{12b}$$

The present formulation allows one to go beyond the use of the long-range part of the potential, made by the sum of charge-induced dipole and dipole-induced dipole interactions:

$$V = -\frac{q^2\alpha}{2r^4} - \frac{2q\alpha\mu\cos\theta}{r^5}, \tag{13}$$

where q is the charge of the ion, μ=3.91 D [29] is its permanent dipole, and α is the polarizability of the noble gas atom. α is 1.64 $\times 10^{-24}$ cm^3 for argon [30] and 0.205 $\times 10^{-24}$ cm^3 for helium [31]. This difference of polarizability makes the situation very different for the two perturbers: the cross section is by far larger for argon than for helium.

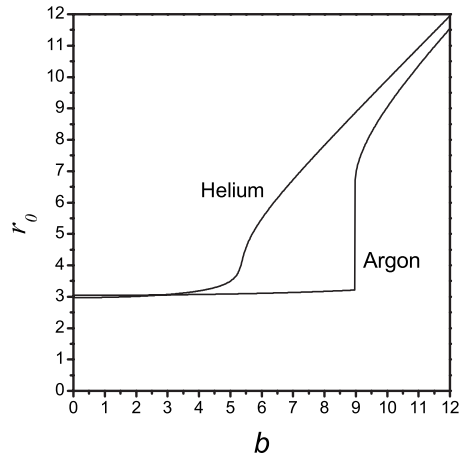

FIG. 1. Dependence of the closest-approach radius r_0 on the impact parameter b. Units are Å. Translation energy is E =67.9 cm^{-1}. The cases HCO$^+$-argon and HCO$^+$-helium are considered. The capture effect occurs for argon but not for helium.

If $V(r)$ is reduced to its long-range part (13), the "middle" term of Eq. (10b) vanishes and Eqs. (10a), (11a), and (12) yield the results of Ref. [26]. The results of Ref. [24] are obtained if straight line trajectories are also assumed.

IV. CAPTURE EFFECT

Figure 1 shows what one gets for the classical relative translation of HCO$^+$-Ar and HCO$^+$-He. The spherical part V_0 of the potential is used and the mean energy at 77 K is assumed. The closest-approach radius r_0 is plotted versus the impact parameter b. For helium one gets a smooth function, while for argon there is a jump at b_c=8.98 Å. When $b<b_c$ there is capture: the two colliding partners approach each other as close as 3 Å. When $b>b_c$ the centrifugal barrier prevents reaching the potential well region. The Langevin [32] approach to capture takes into account only the charge-induced dipole interaction and yields $b_c=(\pi q^2\alpha/2kT)^{1/4}$. For HCO$^+$-Ar this gives b_c=8.65 Å. When a more complete potential is used, including also repulsive terms, capture does not occur for all energy values: it is possible only if the energy is smaller than a critical value E_0, depending on the shape and depth of the potential well. E_0 is 45.3 cm^{-1} for HCO$^+$-He and 456 cm^{-1} for HCO$^+$-Ar. The average energy at 77 K is 67.9 cm^{-1}; hence, capture occurs for argon but not for helium.

In the capture approach only two possibilities are considered: either complete uncorrelation, in capture case, or no relaxation at all. The broadening cross section is equal to capture cross section πb_c^2, while the shift is not obtained. The capture effect can be treated by the sudden adiabatic channel model (SACM), based on quantum mechanics [14–17], which, however, for the case we are considering is very close [26] to the classical result.

V. QUANTUM CALCULATIONS

A quantum calculation of the scattering matrix can be realized by the method implemented by the MOLSCAT computer code. For solving the time-independent Schrödinger equation, this involves expanding the total wave function in the internal basis sets of the colliding species and a partial-wave expansion for the angular part of the collision coordinate. Coupled second-order differential equations are obtained for radial functions which are labeled by the quantum numbers of the asymptotic basis and the partial waves. The coupling, which vanishes asymptotically, is due to the intermolecular potential. Truncation of the infinite asymptotic basis sets leads to the close-coupling method. The scattering matrix is obtained by matching the resulting radial functions at large distances to those which would have been obtained in the absence of an interaction potential.

The rotational energies of the ion are obtained from the literature [33]. As done for semiclassical calculations, the ion is treated as a rigid rotor in its ground vibrational state. Indeed, 803.7 cm^{-1} are needed [34] for the transition to the lowest excited state, 01^10, an energy which is not available.

The total energy E_t and total angular momentum $\boldsymbol{J}$ are constant; E_t is the sum of the asymptotic kinetic energy E and rotation energy E_j of the ion, while $\boldsymbol{J}$ is the sum of the orbital angular momentum $\boldsymbol{L}$ and rotational angular momentum $\boldsymbol{j}$:

$$\boldsymbol{J} = \boldsymbol{L} + \boldsymbol{j}. \tag{14}$$

For a given rotational line $j_f \leftarrow j_i$ and for a given kinetic energy E, the MOLSCAT code calculates the cross section $\sigma_{J_{\min},J_{\max}}$ by taking into account values of J ranging from $J_{\min}$ to $J_{\max}$, which must be given as input. The total cross section σ is obtained by using $J_{\min}=0$ and $J_{\max}$ large enough to provide convergence: $\sigma=\lim_{J_{\max}\to\infty}\sigma_{0,J_{\max}}$.

In Ref. [9] it was observed that the b dependence is not available for quantum cross sections. Strictly speaking, this is true, but something similar to the b dependence, and allowing a closer comparison with semiclassical calculations, can be obtained by defining a partial cross section σ_J. σ_J is not properly defined as $\sigma_{J,J}$—i.e., simply by using $J_{\min}=J_{\max}=J$. Indeed, since in our case the radiation-matter interaction has tensor order 1, σ is not diagonal, but tridiagonal in J. Hence, σ_J is better defined as

$$\sigma_J = \sigma_{0,J} - \sigma_{0,J-1}. \tag{15}$$

The semiclassical impact parameter b is related to L by

$$\hbar L = mvb. \tag{16}$$

For each eigenvalue J of the total angular momentum $\boldsymbol{J}=\boldsymbol{L}+\boldsymbol{j}$, there are several values of L. However, by making an average and by assuming $j \ll L$, one can change Eq. (16) to

$$\hbar J \simeq \hbar L = mvb. \tag{17}$$

Hence, σ_J corresponds to the semiclassical quantity

$$\sigma_J = 2\pi b_J P(b_J)\Delta b, \tag{18}$$

where $b_J=\hbar J/mv$ and $\Delta b=\hbar/mv$.

Equations (15) and (18) allow a detailed comparison between semiclassical and close-coupling calculations. Such a comparison is straightforward when the approximation $J \simeq L$ is good—that is to say, when j is small—but it requires some caution for higher j values.

TABLE I. Comparison between semiclassical (SC) and quantum (Q) cross sections σ for eight rotational lines of HCO^+ perturbed by argon at 77 K temperature. Re σ and $-$Im σ are proportional to the line broadening and line shift, respectively. Units are $Å^2$.

	Re σ		$-$Im σ	
Line	SC	Q	SC	Q
$1\leftarrow 0$	370.7	372.9	41.8	52.8
$2\leftarrow 1$	322.8	314.9	13.5	12.5
$3\leftarrow 2$	279.3	278.6	−0.9	−5.4
$4\leftarrow 3$	257.6	261.6	−3.5	−11.9
$5\leftarrow 4$	253.9	254.1	−1.1	−7.2
$6\leftarrow 5$	253.5	251.3	−0.3	−3.3
$7\leftarrow 6$	253.4	249.3	−0.1	1.0
$8\leftarrow 7$	253.3	247.0	−0.1	−3.2

VI. HCO^+-ARGON

A study of HCO^+-argon at 77 K was performed in Ref. [13] where an accurate potential was obtained and used for the six lowest rotational lines. Quantum calculations were compared to measurements and to ATC results which, because of the restrictions concerning the potential, considered only its long-range part (13). The treatment developed in Sec. III allows us to use the same potential for both theoretical models.

The translation energy was fixed at the 77 K average value: $\bar{E}=4kT/\pi=67.9$ cm^{-1}.

For MOLSCAT calculations a convergence test led us to $J_{\max}=300$. The need for such a high upper limit is related to the long-range nature of the potential: collisions with an impact parameter as large as $b=20-30$ Å still give nonnegligible contributions. With respect to Ref. [13] the rotational lines $j=7\leftarrow 6$ and $8\leftarrow 7$ were added. As a consequence, we found that for converging the scattering matrix it is now necessary to include more rotational energy levels of HCO^+ (up to $j=35$).

A comparison between the two methods is performed in Table I. Agreement is quite good for broadening: the difference is very small and always lower than 2.5%. It is worthwhile noting that for the highest rotational transitions the real cross section is not far from the capture value $\sigma_c=\pi b_c^2=253$ $Å^2$. Indeed, the capture picture of relaxation is reliable at high j, while for the three lowest rotational lines a smaller energy is needed for changing the rotational state and also noncapture collisions contribute to relaxation [26]. For the imaginary part of the cross section the agreement between the two models is acceptable only for the first two lines while it is bad in other cases.

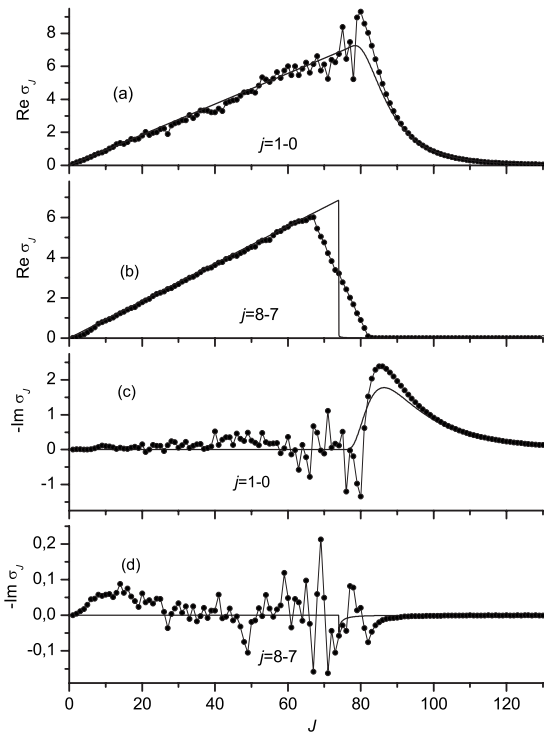

FIG. 2. J dependence of the partial cross section σ_J for HCO^+ perturbed by argon at 77 K. Circles are quantum calculations and solid lines are semiclassical results. Units are $Å^2$.

The dependence on angular momentum is shown in Fig. 2, for sake of brevity only lines $j=1\leftarrow 0$ and $8\leftarrow 7$ are reported. The capture effect is well evident for the line $j=8\leftarrow 7$ in Fig. 2(b). The capture impact parameter $b_c=8.98$ Å corresponds to $J_c\simeq L_c=b_c\sqrt{2mE}/\hbar=74$. At that value of J a rapid transition from very small relaxation to full relaxation (Re $P=1$) occurs. The two calculation models are in very good agreement but for the shape of the transition from capture to noncapture: for quantum calculation the transition is accomplished with a linear trend involving about 15 J values. Indeed, the orbital angular momentum $L=74$ can be obtained for values of J ranging from $L-j$ to $L+j$: just the span observed in Fig. 2(b). Figure 2(a) shows that the capture treatment is not suitable for the line $j=1\leftarrow 0$. In the frame of the ATC approximation Re $P(b)\simeq 1$ holds up to $b\simeq 9.7$—that is to say, $J\simeq 80$. Moreover, the decrease of σ_J for high J values is not as abrupt as in Fig. 2(b). The two methods are in good agreement for both low ($J<60$) and high ($J>90$) values of J. In the intermediate range quantum results exhibit oscillations around the semiclassical value. However, this feature has a small effect on the total cross section σ: an agreement within less than 1% can be seen in Table I.

For the partial shifting cross sections Im σ_J of the line $j=1\leftarrow 0$ [Fig. 2(c)], there is quite good agreement between the two models for weak collisions, while the assumption of a zero shift for strong collisions is rather crude: a not negligible and quite irregular value of Im σ_J is obtained from quantum calculations. As far as the shift of the line $J=8\leftarrow 7$ is concerned [Fig. 2(d)], it is hard to find a correlation between the two methods, but for the fact that the imaginary part Im σ_J of the cross section is far smaller than the real part Re σ_J.

VII. HCO^+-HELIUM

By the potential of Ref. [12] we extended the study to the case of the helium perturber. For MOLSCAT calculations a convergence test led to a J_{max} value depending on the translation energy and going from 60, at low energy, up to 120 at 300 cm^{-1}. Further tests showed that for converging the scattering matrix it is necessary to include rotational energy levels of HCO^+ up to $j_{max}=21$. Both J_{max} and j_{max} are smaller with respect to the case of argon; this reduces the computation time and allowed us to study the energy dependence, to integrate over the thermal distribution at 77 K, and to perform calculations also at room temperature ($T=296$ K, $E=261$ cm^{-1}). The results at 77 K are reported in Table II, while those at room temperature in Table III.

From Tables II and III one can see that for the broadening cross sections, the discrepancies between the two methods

TABLE II. Comparison between semiclassical (SC) and quantum (Q) cross sections σ for eight rotational lines of HCO^+ perturbed by helium at 77 K temperature. Calculations were performed both at mean energy $\bar{E}$ and by explicit integration over the energy distribution. Units are $Å^2$.

	Broadening cross section Re σ				Shift cross section −Im σ			
	Mean energy $\bar{E}$		Integration		Mean energy $\bar{E}$		Integration	
Line	SC	Q	SC	Q	SC	Q	SC	Q
$1\leftarrow 0$	121.3	120.0	126.1	116.0	0.4	2.5	0.7	2.0
$2\leftarrow 1$	118.0	111.0	123.1	111.4	0.8	−0.4	0.9	1.2
$3\leftarrow 2$	113.7	107.9	119.6	107.1	0.9	−0.4	0.7	1.6
$4\leftarrow 3$	109.4	104.2	116.1	103.8	0.6	1.8	0.4	2.1
$5\leftarrow 4$	105.7	99.1	113.3	99.6	0.4	2.9	0.3	2.9
$6\leftarrow 5$	102.9	93.2	111.1	94.9	0.2	3.1	0.1	3.5
$7\leftarrow 6$	101.1	87.7	109.4	90.4	0.1	3.7	0.1	3.6
$8\leftarrow 7$	99.9	83.4	108.1	86.9	0.0	4.3	0.0	3.6

TABLE III. Comparison between semiclassical (SC) and quantum (Q) cross sections σ for eight rotational lines of HCO^+ perturbed by helium at 296 K temperature. Units are $Å^2$.

	Re σ		−Im σ	
Line	SC	Q	SC	Q
$1 \leftarrow 0$	95.6	84.8	0.0	−0.1
$2 \leftarrow 1$	94.5	81.7	0.0	0.0
$3 \leftarrow 2$	93.5	79.8	0.1	−0.1
$4 \leftarrow 3$	92.3	78.1	0.1	0.0
$5 \leftarrow 4$	90.7	76.2	0.1	0.0
$6 \leftarrow 5$	88.7	74.0	0.2	0.1
$7 \leftarrow 6$	86.5	71.7	0.2	0.2
$8 \leftarrow 7$	84.0	69.4	0.2	0.3

range from a few % up to 17%. They are larger for high j values and are of the same order at the two different temperatures considered. From Table II one can see also that for both methods one cannot neglect the difference between the mean energy calculation and integration on a thermal energy distribution.

As far as the shifting cross section is concerned, from Table II one can see that the relative discrepancies between the two methods are very large and tend to increase with j. Absolute discrepancies can be as large as a few % of the broadening value, as in the case of argon. The room-temperature shifts in Table III are too small to allow an analysis; one can just say that both theories forecast a negligible pressure shift.

The energy dependence of the cross sections is reported in Fig. 3 for E ranging from 5 to 300 cm^{-1} and for the lines $j=1 \leftarrow 0$ and $8 \leftarrow 7$. The broadening cross section [Figs. 3(a) and 3(b)] decrease for increasing energy values: at high energy the collision has less time to perturb the rotational state. For quantum cross sections there are oscillations at low energy, which are larger for the line $j=1 \leftarrow 0$. This feature is absent for the semiclassical cross sections which are smooth, but for a small jump at $E=45.3$ cm^{-1}, due to the onset of capture effect. Quantum oscillations extend to the shifting cross sections, reported in Figs. 3(c) and 3(d), and make integration over thermal energy distribution quite tough.

On the whole, no clear evidence is obtained that the agreement between the two methods is better at higher energies, at least for the real part of the cross sections and in the energy range we studied. It would be interesting to check if this unexpected feature is confirmed for other cases. Indeed, there are good reasons for the ATC approximation to become less accurate at low temperature: smaller orbital quantum number L, larger effect on translation of internal energy changes, and larger de Broglie wavelength. All this is probably counterbalanced by larger cross sections, which, as we will discuss in the following, makes the ATC approximation more accurate.

Figures 4 and 5 report the J trend of the partial broadening cross sections σ_J at 296 and 77 K, respectively. Three lines are displayed: $j=1 \leftarrow 0$, $4 \leftarrow 3$, and $8 \leftarrow 7$. For the first rotational line the situation is similar to that found in the case

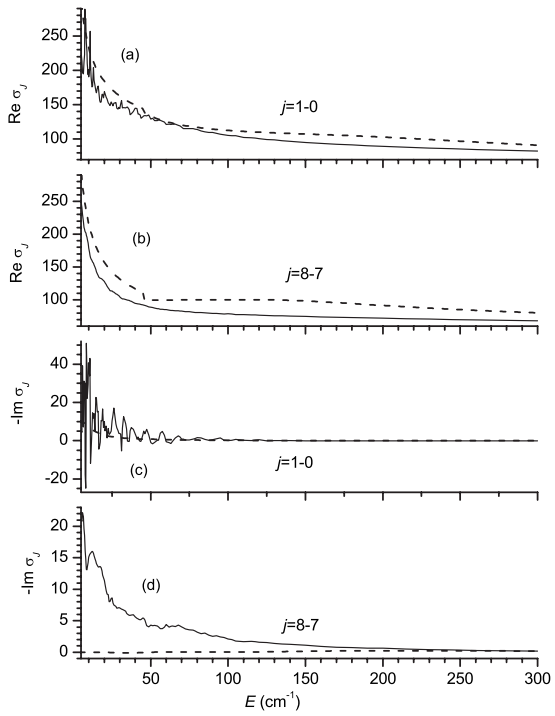

FIG. 3. HCO^+ perturbed by helium. Dependence of the cross section σ on translation energy E. Quantum (solid line) and semiclassical (dashed line) calculations are compared for two rotational lines. Units are $Å^2$.

of the argon perturber. For both low and high J values the ATC approximation is reliable while there is a discrepancy in the interpolation region. Quantum oscillations are present at 77 K [Fig. 5(a)], but almost disappear at 296 K [Fig. 4(a)].

The comparison is more complicated for the other two lines. The assumption $L \gg j$ is less reliable for increasing j values and for decreasing temperatures. The effect of this inaccuracy is small when the trend of σ_J is linear, but it can be large when the slant of the curve has a rapid change. The average on the interval going from $J-j$ to $J+j$ has a small effect in the first case but not in the second. This is what occurred in Fig. 2(b), and this is what occurs, with a decreasing magnitude, in Figs. 5(c), 4(c), 5(b), and 4(b).

VIII. CONCLUSIONS

For eight rotational lines of the HCO^+ ion, perturbed by argon and helium atoms, we compared the collisional line shape parameters obtained by quantum calculations to those obtained by the commonly used semiclassical treatment. We resorted to the same potential for both theoretical approaches. The study was performed at 77 K for argon and at 77 K and 296 K for helium. The dependence of the cross sections on the impact parameter was studied and, for the case HCO^+-He, also the dependence on kinetic energy.

We found an unexpectedly good agreement for both weak (distant) and strong (close) collisions, while in the interpolation region ATC approach meets insoluble difficulties. This confirms what assumed by Anderson in his pioneering paper [3].

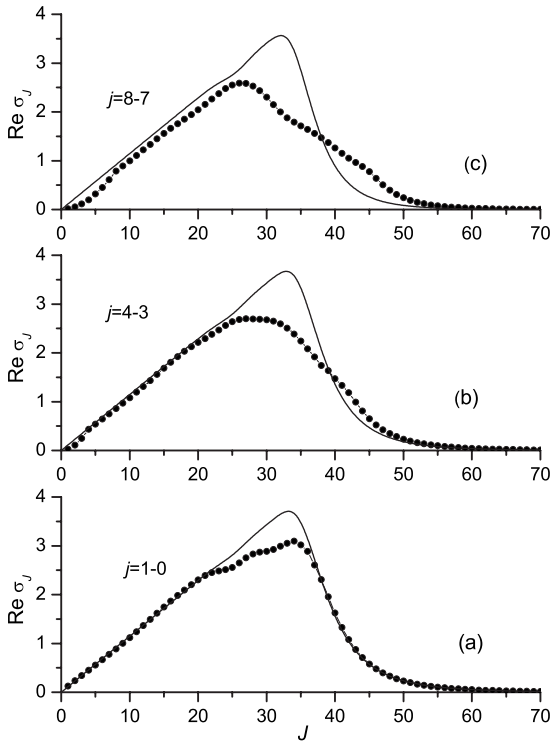

FIG. 4. J dependence of the partial cross section σ_J for HCO^+ perturbed by helium at 296 K. Circles are quantum calculations and solid lines are semiclassical results. Units are Å^2.

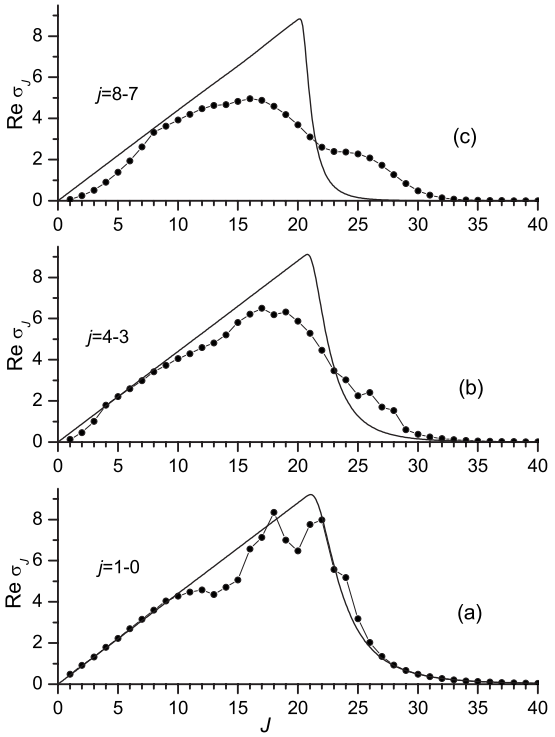

FIG. 5. J dependence of the partial cross section σ_J for HCO^+ perturbed by helium at 77 K. Circles are quantum calculations and solid lines are semiclassical results. Units are Å^2.

The broadening cross sections agree within 2.5% for the argon perturber and within 17% for the helium perturber. Why a so different accuracies? The masses of the two atoms differ by a factor of 10, yielding a factor of 4.8 for the reduced mass m of the colliding pair. By looking only at the 77 K data one could conclude that the difference should be ascribed to the de Broglie wavelength. Indeed, the semiclassical approximation is commonly assumed to be reliable only when the de Broglie wavelength $\lambda = h/\sqrt{2mE}$ is much smaller than the length scale of variation of the potential. At 77 K λ is 0.76 Å for argon and 1.67 Å for helium. For both cases, but especially for helium, the potential changes within one de Broglie wavelength are large, and this could explain the discrepancy. However, for helium at room temperature λ is 0.85 Å, close to the value for argon at 77 K; nevertheless, the accuracy of the semiclassical calculation is still bad. We think that the explanation lies probably more in the difference of polarizability than in the difference of mass. Argon is 8 times more polarizable than helium and this makes the long-range tail of the potential 8 times larger. The reliability of the ATC method depends on how accurately it describes the transition, for decreasing impact parameter, from small to full relaxation. This occurs at distances of the order of the so-called microwave radius $r_{mw} = \sqrt{\mathrm{Re}\,\sigma/\pi}$, which depends on the rotational line and, for those we considered, ranges from 8.9 to 10.9 Å for argon, from 5.2 to 6.2 Å for helium at 77 K, and from 4.7 to 5.2 Å for helium at 296 K. Smaller r_{mw} values mean closer collisions, more poorly described by the semiclassical approximation. It is mainly this feature that probably accounts for the better accuracy in the case of argon and also for the fact that for helium the accuracy is not much increased by changing the temperature from 77 to 296 K.

For the shifting cross sections an acceptable agreement was found only when the shift/broadening ratio is not too small. On the whole, we can conclude that semiclassical shift calculations are accurate within a few % of the broadening value.

Quantum calculations exhibit resonances both for the dependence on impact parameter and on kinetic energy. The oscillations for energy dependence were discussed by Ball and De Lucia [35]. For CO perturbed by helium at temperatures below 10 K they compared broadening and state-to-state cross sections, concluding that some of the peaks in the broadening are due to inelastic (state changing) collisions while other to elastic (phase changing) processes. Our calculations for the case HCO^+-He show that the oscillations extend also to the shifting cross section. The resonances are less evident at high j; as supposed in Ref. [35], this must be probably ascribed to the larger energy needed to excite rotational transitions. Indeed, for changing the lower state of the line $j=1\leftarrow 0$ [Figs. 3(a) and 3(c)] only 3 cm^{-1} are needed, while 21 cm^{-1} are required for the line $j=8\leftarrow 7$ [Figs. 3(b) and 3(d)].

Quantum oscillations were found as well in the trend of the partial cross section σ_J; they do not have a large influence on the total cross section σ and are larger in the interpolation region, between strong and weak collisions. Such oscillations are probably due to the interference between different paths, a feature that the usual semiclassical calcula-

tions do not account for. For the case of helium perturber these resonances almost disappear at room temperature, probably because translation energy is larger than the depth of potential well.

ACKNOWLEDGMENT

The author thanks Jeremy M. Hutson for explanations of MOLSCAT.

[1] A. M. Arthurs and A. Dalgarno, Proc. R. Soc. London, Ser. A **256**, 540 (1960).
[2] J. M. Hutson and S. Green, MOLSCAT computer code, version 14 (1994), distributed by Collaborative Computational Project No. 6 of the Science and Engineering Research Council (UK) (http://www.giss.nasa.gov/tools/molscat/).
[3] P. W. Anderson, Phys. Rev. **76**, 647 (1949).
[4] C. T. Tsao and I. Curnutte, J. Quant. Spectrosc. Radiat. Transf. **2**, 41 (1962).
[5] A. Di Giacomo and O. Tarrini, Nuovo Cimento B **62**, 1 (1969); **68**, 165 (1970).
[6] B. S. Frost, J. Phys. B **9**, 1001 (1976).
[7] J. S. Murphy and J. E. Boggs, J. Chem. Phys. **47**, 691 (1967); **50**, 3320 (1969).
[8] D. Robert and J. Bonamy, J. Phys. (Paris) **40**, 923 (1979).
[9] J. M. Hartmann and C. Boulet, J. Chem. Phys. **113**, 9000 (2000).
[10] J. M. Hutson, in *Status and Future Developements in the Study of Transport Properties*, edited by W. A. Wakeman *et al.* (Kluwer Academic, Dordrecht, 1992).
[11] W. B. Neilsen and R. G. Gordon, J. Chem. Phys. **58**, 4131 (1973); **58**, 4149 (1973).
[12] T. Monteiro, Mon. Not. R. Astron. Soc. **210**, 1 (1984).
[13] G. Buffa, L. Dore, F. Tinti, and M. Mewley, ChemPhysChem **7**, 1764 (2006).
[14] J. Tröe, J. Phys. Chem. **90**, 3485 (1986); J. Chem. Phys. **87**, 2773 (1987).
[15] Q. Liao and E. Herbst, Astrophys. J. **444**, 694 (1995).
[16] Q. Liao and E. Herbst, J. Chem. Phys. **104**, 3956 (1996).
[17] M. Quack and J. Troe, in *Statistical Adiabatic Channel Model, in Encyclopedia of Computational Chemistry*, edited by P. Von Raguè Schleyer (Wiley, New York, 1998).
[18] M. Baranger, Phys. Rev. **111**, 481 (1958); **111**, 494 (1958); **112**, 855 (1958).
[19] U. Fano, Phys. Rev. **131**, 259 (1963).
[20] R. M. Herman, Phys. Rev. **132**, 262 (1963); J. Quant. Spectrosc. Radiat. Transf. **3**, 449 (1963).
[21] A. Di Giacomo and O. Tarrini, Nuovo Cimento B **68**, 165 (1970).
[22] C. Boulet, D. Robert, and L. Galatry, J. Chem. Phys. **65**, 5302 (1976).
[23] Krishnaji and S. L. Srivastava, J. Chem. Phys. **41**, 2266 (1964); **42**, 1546 (1965).
[24] G. Buffa, O. Tarrini, G. Cazzoli, and L. Dore, Phys. Rev. A **49**, 3557 (1994).
[25] B. Labani, J. Bonamy, D. Robert, J. M. Hartmann, and J. Taine, J. Chem. Phys. **84**, 4256 (1986).
[26] G. Buffa, O. Tarrini, G. Cazzoli, and L. Dore, J. Chem. Phys. **111**, 1870 (1999).
[27] A. D. Bykov, N. N. Lavrent'eva, and L. N. Sinitsa, Atmos. Oceanic Opt. **5**, 587 (1992); **5**, 728 (1992).
[28] J. Buldyreva, J. Bonamy, and D. Robert, J. Quant. Spectrosc. Radiat. Transf. **62**, 321 (1999).
[29] P. Botschwina, in *Ion and Cluster Ion Spectroscopy and Structure*, edited by J. P. Maier (Elsevier, Amsterdam, 1989).
[30] C. G. Gray and K. E. Gubbins, *Theory of Molecular Fluids* (Clarendon Press, Oxford, 1984), Vol. 1.
[31] G. Łach, B. Jeziorski, and K. Szalewicz, Phys. Rev. Lett. **92**, 233001 (2004).
[32] P. Langevin, Ann. Chim. Phys. **5**, 245 (1905).
[33] G. A. Blake, K. B. Laughlin, R. C. Cohen, K. L. Busarow, and R. J. Saykally, Astrophys. J., Lett. Ed. **316**, L45 (1987).
[34] C. Puzzarini, R. Tarroni, P. Palmieri, S. Carter, and L. Dore, Mol. Phys. **87**, 879 (1996).
[35] C. D. Ball and F. C. De Lucia, Phys. Rev. Lett. **81**, 305 (1998).